

Tamm states and nonlinear surface modes in photonic crystals

Steven K. Morrison ^{*,a} and Yuri S. Kivshar ^a

^a*Nonlinear Physics Center and Center for Ultra-high bandwidth Devices for Optical Systems (CUDOS), Research School of Physical Sciences and Engineering, Australian National University, Canberra ACT 0200, Australia*

Abstract

We predict the existence of surface gap modes, known as Tamm states for electronic systems, in truncated photonic crystals formed by two types of dielectric rods. We investigate the energy threshold, dispersion, and modal symmetries of the surface modes, and also demonstrate the existence and tunability of *nonlinear Tamm states* in binary photonic crystals with nonlinear response.

Key words: Surface modes, Tamm states, photonic crystals

PACS: 73.20.-r, 42.70.Qs, 42.65.-k

1 INTRODUCTION

Surface modes are a special type of wave localized at the interface separating two different media. In periodic systems, the modes localized at the surfaces

* Tel.: +61 261258277; Fax.:+61 261258588

Email address: `skm124@rsphysse.anu.edu.au` (Steven K. Morrison).

are known as Tamm states [1], first found as localized electronic states at the edge of a truncated periodic potential. Surface states have been studied in different fields of physics, including optics [2], where such waves are confined to the interface between periodic and homogeneous media.

Photonic crystals, artificially fabricated periodic structures with bandgap spectra [3], can be used for controlling the properties of light in different devices including dielectric mirrors and waveguides. In many such applications, photonic crystals are finite, and are terminated at surfaces where electromagnetic waves are significantly affected by the breaking of the translational invariance by the underlying periodic structure.

Although the properties of electromagnetic waves in bulk photonic crystals are well understood, studies of electromagnetic waves near the surfaces of photonic crystals are relatively limited and, unlike electronic Tamm states, a truncated photonic crystal does not always support surface states [4]. Surface states in photonic crystals have only been shown to exist under appropriate changes to the surface layer, such as a termination through the surface cell or a change to the surface geometry or material properties [5,6,7]. Furthermore, such surface waves are known to be significantly sensitive to the surface termination [6,8].

In this Communication, we study surface waves in photonic crystals with terminated (but not altered) surface structures. For the first time to our knowledge, we show the existence of strongly localized surface modes in binary photonic crystals, in a complete analogy to Tamm states in electronic systems. Our analysis of the linear properties of the diatomic structure illustrates the dispersion relations and field localization of the surface states, and the subsequent influence of variations to the crystal geometry. Additionally,

we study the nonlinear behavior of the surface states when the dielectric function of the photonic crystal includes a Kerr style nonlinearity, and discuss the nonlinearity-induced tunability of nonlinear Tamm surface states.

2 Model and numerical methods

We consider the propagation of the TM-polarized waves in a two-dimensional *binary photonic crystal* formed by two square lattices of larger and smaller dielectric rods, as shown in Fig. 1(a), where r_a and r_b are the rod radii populating the lattices. These two elemental lattices merge to form a single lattice of period a , with a unit cell created by a single, large rod at the center of the cell and a single small rod distributed as four quadrants at the corners of the cell; thereby forming a unit cell with two rods. In general, the binary structure reduces the geometric symmetries of the photonic crystal, thereby lifting the degeneracies of some of the crystal states [9]. However, the structure we study here does not possess this capacity and as such maintains the C_{4v} point group symmetry of the constituent square lattices.

We consider the surface termination that has translational symmetry along the surface where a row of either large radius rods r_a or small radius rods r_b form the surface layer exclusively. In all cases discussed below only complete rods are considered within the surface layers, similar to the original context of Tamm states.

For these binary crystals, we set the radius of the rods as $r_a = 0.21a$ and $r_b = 0.13a$. The dielectric rods of the photonic crystal correspond to high potential optical regions. In this study, we set the linear dielectric constant of

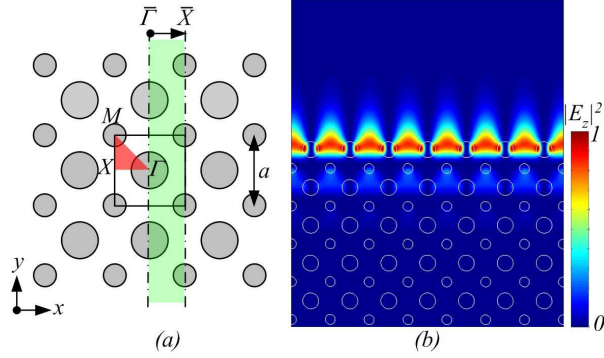


Fig. 1. (a) Structure of a binary photonic crystal with a surface termination. Shadings (red and green) show the equivalent irreducible Brillouin zone of an infinite and semi-infinite photonic crystal projected onto the crystal geometry. (b) Spatial profile of the linear surface mode as the color plot of $|E_z|^2$.

the rods to $\varepsilon_r = 11.56$, corresponding to AlGaAs at a wavelength of $1550nm$, and assume negligible losses.

To analyze the surface states, we employ two complementary numerical methods: the plane wave expansion method (PWE) [10,11] and the finite-difference time-domain method (FDTD) [12,13]. Due to the normal computational intensive nature of the FDTD method and the need to reduce the time step to maintain numerical stability [14] for the nonlinear case, the method is extremely time consuming. To reduce this burden, we model a semi-infinite crystal using a supercell representation [15,13] that has a transverse size of one unit cell, and contains nine unit cells of the photonic crystal, including the surface cell, and nine unit cells of vacuum in the lateral direction. The supercell is bordered by a perfectly matched layer [16]. The boundaries perpendicular to the surface are periodic, and configured with a π spatial phase shift that sets the wave vector to the edge of the surface Brillouin zone.

The supercell is excited using a two-dimensional Gaussian pulse, centrally located within the spatial domain and the photonic band gap, that energizes

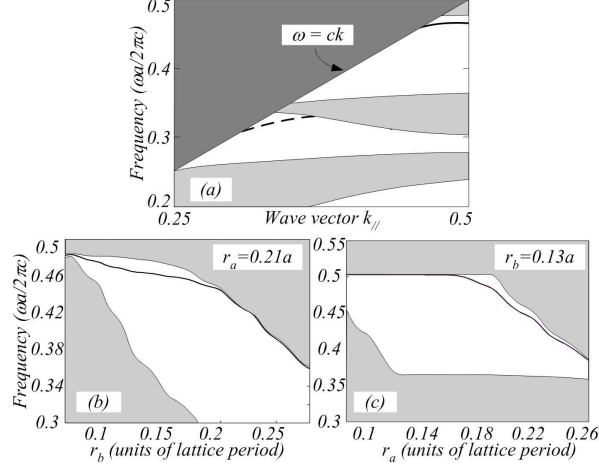


Fig. 2. (a) Surface mode dispersion relationships for the surface formed by larger (upper solid line) and smaller (lower dashed line) rods. (b,c) Photonic band gap and surface mode frequencies with respect to dielectric rod radii. In (b) the larger rods of radius r_a are held constant while the radius r_b of the smaller rods is varied, whereas in (c) the smaller rods of radius r_b are held constant while the radius r_a of the larger rods is varied.

the resonant modes of the crystal and the surface structures. A discrete Fourier transform of the time evolution data, recorded at the surface of the photonic crystal, is used to determine the spectral response of the surface states. In a similar manner, the spatial mode profile is calculated from the time evolution data of the full simulation domain at the peak frequency of the surface state.

3 Linear Tamm states

For the linear surface states, the dispersion relationships are presented in Fig. 2(a). The dark grey region within the dispersion diagrams depicts the continuum of free-space states that exist above the line light ($\omega = ck$) that are not bound to the surface. Light grey regions within the diagram indicate the Bloch states of the infinite photonic crystal; states within these regions

can couple into the crystal, and again are not bound to the surface.

Surface states are formed within the second photonic bandgap of the infinite crystal, and are shown with a solid black line in the diagram. The surface states occur within the second band gap when the surface is terminated in a row of large rods of radius r_a . A localized surface state can form within the first bandgap when the crystal is terminated in a row of smaller rods, as indicated by the dashed line in Fig. 2(a). This state, however, can couple to the Bloch states of the infinite crystal, and we do not consider it in detail.

We analyze the characteristics of the surface states by varying the radii of the constituent rods of the photonic crystal. Figures 2(b,c) show the influence of the rod radii on the bandgap edges and surface state frequencies. The larger rods principally define the upper bandgap edge for the $\Gamma - X$ direction and have virtually no effect on the lower bandgap edge, whereas the smaller rods set the lower bandgap edge with very weak effect on the upper bandgap edge. Figures 2(b,c) also confirm that the surface mode does not exist when the radii of the two constituent rods are equal

The consistency of the location of the surface states within the bandgaps signifies the states existence domain is predominantly defined by the crystal geometry; a feature attributed to the binary nature of the crystal, which has previously been shown to provide robust spectral features in the presence of geometric variations [9]. The spatial field localizations can be understood by noting the symmetries of the Bloch waves above and below the bandgap. In the $\Gamma - X$ direction below the second bandgap, the Bloch wave symmetries place the electric field within the smaller rods, whereas for above the bandgap the field resides between the rods in free-space, with some overlap into the

larger rods. As the surface is formed by large rods and the states are near the upper bandgap edge, they take on the Bloch mode symmetries of this frequency region.

4 Nonlinear Tamm states

We study the properties of nonlinear surface states through the addition of a third-order susceptibility term within the polarization field of all rods. Throughout our analysis we only modify the $\chi^{(3)}$ coefficient and maintain the input field intensity and density. Under steady-state conditions, the principal effect of the nonlinear term is to induce an intensity dependent change to the dielectric strength of the surface rods. Simulations of the nonlinear dielectric rods of the photonic crystals are performed using the FDTD method [17,12]. This is achieved by adding a $\chi^{(3)}$ term to the polarization as: $\mathbf{P} = \chi^{(1)}\mathbf{E} + \chi^{(3)}|\mathbf{E}|^2\mathbf{E}$. The analysis of the linear surface states revealed that the field intensity varies appreciably across the surface rods. For the nonlinear surface rods this causes an equivalent change in the dielectric constant. In our analysis of the nonlinear surface states we consider only a focussing nonlinearity ($\chi^{(3)} > 0$) that results in localized increases in the dielectric index which are proportional to the cube of the electric field. In turn, this leads to a decrease in the resonant frequency of the surface state.

Figure 3(a) illustrates the surface mode frequency shift as the strength of the third-order susceptibility grows. A strong frequency shift is observed for moderate changes in $\chi^{(3)}$, with a threshold to the onset of strong frequency shifting at approximately $\chi^{(3)} = 1 \times 10^{-3} \mu m^2/V$. These $\chi^{(3)}$ values exemplify the significant dynamic range of the nonlinear surface state of a binary pho-

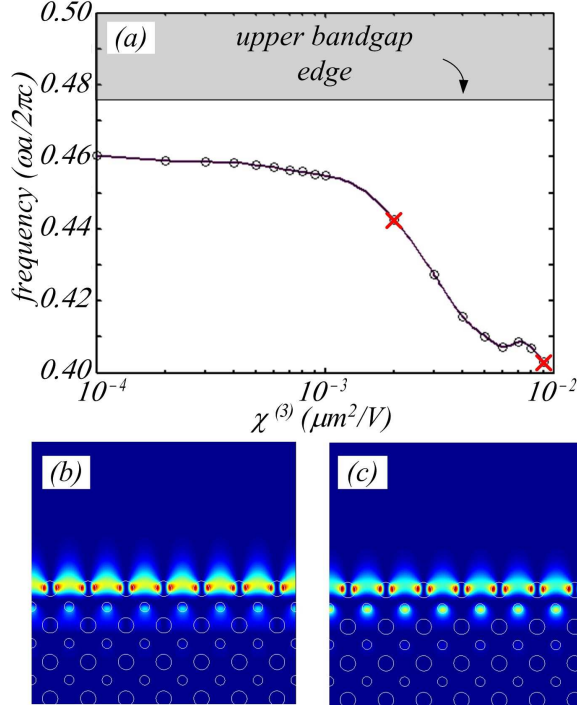


Fig. 3. (a) Nonlinear frequency shift of the surface state vs. the nonlinear susceptibility for $r_a = 0.21a$ and $r_b = 0.13a$; (b,c) Spatial profile of the surface modes as the color plots of the field density $|E_z|^2$ for $\chi^{(3)} = 2 \times 10^{-3} \mu\text{m}^2/V$ (left), and $\chi^{(3)} = 9 \times 10^{-3} \mu\text{m}^2/V$ (right).

tonic crystal using realistic nonlinearities; for example a typical value of $\chi^{(3)}$ for AlGaAs is $\chi^{(3)} = 8.2 \times 10^{-3} \mu\text{m}^2/V$ [18].

The distinct spatial field profile of the surface state, and its dramatic change with dielectric strength leads to the strong $\chi^{(3)}$ sensitivity. This is demonstrated in Fig. 3(b,c), which shows the spatial field profiles for (b) $\chi^{(3)} = 2 \times 10^{-3} \mu\text{m}^2/V$, and (c) $\chi^{(3)} = 9 \times 10^{-3} \mu\text{m}^2/V$. In a homogeneous nonlinear focusing medium, a nonlinearity-induced change in the dielectric constant results in a greater localization of the light, which under appropriate conditions can lead to *spatial surface solitons*. However, for the surface state of the binary photonic crystal, the increased dielectric constant causes the conditions for the surface resonance to diminish, resulting in a reduction in the field

localization, leading to a complex balance between the nonlinearity and surface interaction. In general, as the nonlinear surface state evolves and reaches steady state conditions, the field intensity within the surface rods reduces. This effect provides optical limiting that prevents saturation of the nonlinearity and unrealistic changes to the dielectric strength. Additionally, the competing effects due to nonlinearity and the surface can lead to complex behavior, as seen for $\chi^{(3)} = 7 \times 10^{-3} \mu m^2/V$ where the frequency of the surface state increases. Another consequence of the nonlinear surface structure is the formation of a near-surface defect state, as seen in Fig. 3(c), where the localized state forms in the neighboring row of small rods.

Recent studies have demonstrated the application of optical surface states of photonic crystals for guiding light, the formation of high-quality micro cavities, and sub-wavelength imaging [19,20,21]. We expect that the nonlinear tunable Tamm states found here would provide substantial nonlinearity-induced control within these applications leading to novel all-optical surface devices such as optical limiters and switches.

5 Conclusion

In conclusion, we have predicted the existence of surface Tamm states in binary two-dimensional photonic crystals. Using nonlinear surface rods, we have highlighted the dynamic tunability of the surface states resulting from the unusual spatial distribution of the surface mode, and its geometric transformation through a competition of the nonlinearity and surface effects.

Acknowledgment

This work was produced with the assistance of the Australian Research Council under the ARC Centres of Excellence program.

References

- [1] I.E. Tamm, *Z. Phys.* **76**, 849 (1932).
- [2] P. Yeh, A. Yariv, and A.Y. Cho, *Appl. Phys. Lett.* **32**, 102 (1978).
- [3] J. D. Joannopoulos, R. D. Meade, and J. N. Winn, *Photonic Crystals* (Princeton University, Princeton, 1995).
- [4] X. Yi, P. Yeh, J. Hong, S. Fan, and J. D. Joannopoulos, (QTuG6), p. 85, In: *Proceeding of QELS*, 2000.
- [5] R. D. Meade, K. D. Brommer, A. M. Rappe, and J. D. Joannopoulos, *Phys. Rev. B* **44** 10961 (1991).
- [6] W. M. Robertson, G. Arjavalingam, R. D. Meade, K. D. Brommer, A. M. Rappe, and J. D. Joannopoulos, *Opt. Lett.* **18**, 528 (1994).
- [7] F. Ramos-Mendieta and P. Halevi, *J. Opt. Soc. Am. B*, **14**, 370 (1997); *Phys. Rev. B* **59**, 15112 (1999).
- [8] Y. A. Vlasov, N. Moll, and S. J. McNab, *Opt. Lett.* **29**, 2175 (2004).
- [9] C. M. Anderson and K. P. Giapis, *Phys. Rev. Lett.* **77**, 2949 (1996).
- [10] K. Sakoda, *Optical Properties of Photonic Crystals* (Springer-Verlag, Berlin, 2001).
- [11] S. G. Johnson and J. D. Joannopoulos, *Optics Express* **8**, 173 (2000).

- [12] A. Taflove, *Computational Electrodynamics. The Finite-Difference Time-Domain Method* (Artech House, Norwood, 1995).
- [13] T. Baba, *Roadmap on Photonic Crystals* (Kluwer, Dordrecht, 2003).
- [14] R. F. Remis, *J. Comp. Phys.* **163**, 249 (2000).
- [15] C. T. Chan, Q. T. Yu, and K. M. Ho, *Phys. Rev. B*, **51**(23), 16635 (1995).
- [16] J. P. Berenger, *Comp. Phys.* **114**, 185 (1994).
- [17] R. M. Joseph and A. Taflove, *IEEE Trans. Ant. and Prop.* **45** 364 (1997).
- [18] M. Bahl, N. Panoiu, and R. M. Osgood Jr., *Phys. Rev. E*, **67**, 056604 (2003).
- [19] J. Yang, S. Kim, G. Kim, H. Park, and Y. Lee, *Appl. Phys. Lett.* **84**, 3016 (2004).
- [20] S. Xiao and M. Qiu, *Appl. Phys. Lett.* **87**, 111102 (2005).
- [21] Li. Chengyu , J. M. Holt, and A. L. Efros *J. Opt. Soc. Am. B.* **23**, 490-497 (2006).